Journal of Drug Delivery Science and Technology 60 (2020) 101931

Contents lists available at ScienceDirect

Journal of Drug Delivery Science and Technology

journal homepage: www.elsevier.com/locate/jddst

Research paper

A simple desolvation method for production of cationic albumin nanoparticles with improved drug loading and cell uptake

Sumeyra Cigdem Sozer [a], Tugce Ozmen Egesoy [a], Merve Basol [b,c], Gulcin Cakan-Akdogan [b], Yasar Akdogan [a,*]

[a] Materials Science and Engineering Department, Izmir Institute of Technology, Izmir, 35430, Turkey
[b] Izmir Biomedicine and Genome Center, Izmir, 35340, Turkey
[c] Izmir International Biomedicine and Genome Institute, Dokuz Eylul University, Izmir, 35340, Turkey

ARTICLE INFO

Keywords:
Cationic albumin nanoparticles
Desolvation
Salicylic acid
Drug loading
Cell uptake

ABSTRACT

The transport protein albumin has been used as a drug nanocarrier for a long time due to its versatility. Albumin is negatively charged at physiological conditions limiting its anionic drug loading capacity. However, loading of anionic drugs in the albumin nanoparticles (NPs), can be facilitated by albumin cationization. Here, we postulate a simple desolvation method for preparation of cationic albumin NPs with improved anionic drug loading. First, bovine serum albumin was cationized with ethylenediamine. Next, salicylic acid (SA) was added to the cationic bovine serum albumin (cBSA) solution prior to the desolvation. Among different desolvating agents tested, acetonitrile allowed the highest nanoparticle formation yield. The SEM analyses showed that the average size of cBSA NPs decreased from ~200 nm to ~100 nm upon SA loading. Moreover, the drug loading capacity of cBSA NPs was found to increase ~2 fold, and drug release was slower compared to BSA NPs. Finally, a significant increase in cellular uptake of cBSA NPs compared to that of native BSA NPs showed the potential for improved drug delivery.

1. Introduction

Poor drug solubility is one of the most important challenges the pharmacology is facing. Various techniques are employed to achieve increased drug solubility [1–3]. Among them, loading of drugs in nanocarriers is a preferred choice providing long term stability in addition to enhanced solubility [4]. Albumin protein has been widely used to prepare nanocarriers for drug delivery [5,6].

Human serum albumin (HSA) is the most abundant protein in human blood with a concentration of about 40 mg/mL [7]. Every day, 13–14 g of albumin is synthesized in the liver and released to the circulation [8]. Serum albumin is the natural carrier of a large number of drugs transporting them from the bloodstream to target cells [9–11]. Notably, cancer drugs associated with albumin are found to accumulate in cancer cells through the receptor-mediated albumin uptake pathways [12,13]. Therefore, albumin attracts great interest in the pharmaceutical industry, as a drug carrier.

Drug-albumin formulations have been classified into three main groups; non-covalent associations, covalent binding and drug loading in albumin nanoparticles (NPs) [7]. Drug-loaded albumin NPs have advantages over the other formulation methods. For example, drugs loaded in albumin NPs are protected until the NP reaches the therapeutic site of interest, where they can be released slowly in a controlled (sustained) manner [14]. In addition, site-specific delivery of drugs can be achieved by coupling of targeting ligands to NP surface [15]. Moreover, NPs with high carrier capacity can be taken orally or by inhaler [16]. These features of NPs improve the efficiency of drugs without increasing the drug dose and dosage frequency.

Emulsification and desolvation are two main methods of albumin NP preparation. In the emulsification method, the albumin aqueous solution is emulsified in immiscible liquids such as dichloromethane, cyclohexane or ionic liquids by using a high-pressure homogenizer, a high-speed homogenizer or an ultrasonic shear in the presence of surfactant molecules [17–22]. In the desolvation method, addition of a desolvating agent, such as ethanol or acetone, decreases the hydration level and the solubility of the albumin, leading to NP formation [23,24]. Optimization of the NP preparation process by adjusting the type of solvent, solvent addition rate, albumin concentration, pH, temperature and ionic

* Corresponding author.
E-mail address: yasarakdogan@iyte.edu.tr (Y. Akdogan).

https://doi.org/10.1016/j.jddst.2020.101931
Received 30 April 2020; Received in revised form 4 July 2020; Accepted 12 July 2020
Available online 8 August 2020
1773-2247/

strength of the medium is used for controlled aggregation of albumin, yielding dispersed spherical albumin NPs in the presence of a cross-linker e.g. glutaraldehyde [23–30].

In the desolvation method, drug loading of albumin NPs depends on the interactions such as hydrogen bonding, electrostatic and hydrophobic interactions between albumin and drugs [31]. Although albumin surface is negatively charged at physiological condition pH = 7.4, both neutral and negatively charged drugs can bind to albumin [32]. In our previous studies, we showed that a maximum of 7 spin labeled salicylic acid (SA) molecules which are negatively charged at pH = 7.4 can bind to each bovine serum albumin (BSA) protein [33]. However, SA binding to a cationic BSA (cBSA) protein is much more efficient, yielding almost 20 spin labeled SAs per one cBSA molecule [34]. This demonstrates the strong effect of electrostatic interactions in the drug-protein conjugation.

The NPs with positively charged groups have been shown to bind the negatively charged groups on cell surfaces, such as sialic acid, which initiate cell uptake [35]. In the literature, different methods have been developed to prepare cationic albumin NPs. Abbasi et al. prepared Doxorubicin (Dox) loaded cHSA NPs by coating anionic HSA NPs with positively charged polyethylenimine (PEI) through the electrostatic binding [36]. In another study, BSA was conjugated with fatty amines to form hydrophobic cBSA NPs in an aqueous medium [37]. Han et al. prepared cBSA proteins via ethylenediamine conjugation, and prepared self-assembled cBSA NPs by mixing cBSA with siRNA which interact with each other electrostatically [38]. Byeon et al. prepared Dox loaded cHSA NPs with an emulsification method using a high-pressure homogenizer after surface modification of HSA with ethylenediamine [31].

Herein, cBSA NPs were prepared with a simple desolvation method. Obtained cBSA NPs were shown to have increased drug loading capacity, slower drug release and increased cellular uptake when compared to the native albumin NPs. To our knowledge this is the first study to prepare cationic albumin NPs by the simple desolvation technique. First, we prepared cBSA proteins by conjugation of ethylenediamine to BSA, and then desolvating agents were added into the cBSA aqueous solution in the presence of glutaraldehyde to prepare cBSA NPs. Depending on the type of desolvating agent, the yield of cBSA NPs formation changed dramatically. For investigating the drug loading capacity, salicylic acid (SA) was used as a model anionic drug. cBSA NPs were loaded with SA through the desolvation process. The drug entrapment efficiency, drug loading and drug release properties of cBSA NPs were investigated and compared with those of non-modified BSA NPs. Also, the effects of surface cationization on the cell uptake efficiency and cytotoxicity were evaluated.

2. Experimental

2.1. Materials

Bovine serum albumin (BSA, Mw: 66.5 kDa lyophilized powder, >96%), N-(3-Dimethylaminopropyl)-N′-ethylcarbodiimidehydrochloride (EDC), ethylenediamine (EDA), glutaraldeyhde solution (8% (v/v) in H_2O), methanol, ethanol, propanol, isopropanol, acetone, salicylic acid, albumin-fluorescein isothiocynate conjugate (FITC), dimethyl sulfoxide (DMSO) were purchased from Sigma – Aldrich. Acetonitrile was purchased from Merck. The pH of the ethylenediamine solution was adjusted with hydrochloric acid (6 M) solution.

2.2. Preparations

2.2.1. Preparation of cationic bovine serum albumin (cBSA) protein

cBSA was prepared as previously described in our publication and elsewhere [39,40]. 100 mg BSA was dissolved in 1 mL of deionized water. 650 μL ethylenediamine was mixed with 500 μL deionized water, and then the solution pH was adjusted to 4.75 by addition of 9 mL HCl (6 M). The BSA solution was added to the ethylenediamine solution. 14.5 mg EDC was dissolved in 15 μL deionized water, then it was slowly added to the BSA-ethylenediamine solution. The reaction was stirred at 750 rpm for 2 h. The reaction was stopped by the addition of 4 M acetate buffer (pH 4.75). cBSA was purified by 0.1 M aceate buffer and deionized water for the elimination of excess amount of EDC and ethylenediamine by 3 cycles of centrifugation using centrifugal filter (molecular cut off: 50 kDa) (13,000 rpm, 3 min). The final cBSA was collected from centrifugal filter, and then it was lyophilized and stored at 4 °C. The cBSA yield was 70%. Fluorescein isothiocynate conjugated cBSA (FITC-cBSA) protein was prepared similar to the procedure used in the preparation of normal cBSA but with FITC-BSA instead of BSA.

2.2.2. Preparation of cBSA NPs and BSA NPs

cBSA NPs and BSA NPs were synthesized by the desolvation method with using different desolvating agents, and cross-linked by glutaraldeyhde. Methanol, ethanol, propanol, isopropanol, acetone and acetonitrile were tested as desolvation agents. Briefly, 62.5 mg cBSA (or BSA) was dissolved in 1 mL deionized water for 20 min. The desolvating agent was added dropwise to cBSA (or BSA) solution using a syringe pump with a flow rate of 1.0 mL/min. The NPs were formed under 750 rpm continuous stirring. The cBSA aqueous solution did not turn turbid upon addition of 1:6 (v/v) of methanol or 1:6 (v/v) of ethanol; turned slightly turbid upon addition of 1:5 (v/v) of propanol, 1:5 (v/v) of isopropanol or 1:4 (v/v) of acetone. The most turbid cBSA solution was obtained by adding 1:4 (v/v) of acetonitrile. Then, 18 μL of 8% (v/v) cross-linking agent glutaraldeyhde was added to each reaction. On the other hand, the BSA aqueous solutions turned turbid quicker by adding the desolvating agents. Yet, 1:6, 1:4, 1:3, 1:3, 1:4 and 1:4 (v/v) of methanol, ethanol, propanol, isopropanol, acetone and acetonitrile were added to the BSA solution to have similar conditions with cBSA experiments. The NPs were stirred overnight at 750 rpm to increase the stability of the NPs by crosslinking entirely. Aliquots NP solutions were precipitated by centrifugation at 14,000 rpm for 45 min. Pellets were washed with distilled water to eliminate desolvating agents, unreacted cBSA, BSA and glutaraldeyhde. FITC-cBSA NPs and FITC-BSA NPs were prepared similar to the procedures used in the preparation of cBSA NPs and BSA NPs, but with FITC-cBSA and FITC-BSA, respectively.

2.3. Characterization of cBSA proteins, cBSA NPs and BSA NPs

The zeta potential and molecular weight of cBSA and BSA were characterized in distilled water by a Malvern dynamic light scattering (DLS) Nano-ZS instrument (Worcestershire, UK) and a mass spectrometer using Bruker Autoflex-III (smartbeam) MALDI TOF/TOF system, respectively. cBSA and BSA aqueous solutions were measured by attenuated total reflectance Fourier transform infrared (ATR-FTIR) spectrometer (Perkin Elmer) with a resolution of 4 cm-1 cBSA and BSA aqueous solutions were measured before and after addition of acetonitrile with a Varian Cary Eclipse Fluorescence spectrophotometer equipped with 1.0 cm path length quartz cuvettes.

After the purification of NPs, pellets were lyophilized for the yield calculations. Lyophilized NPs were dissolved in distilled water for the size and zeta potential measurements. The size and shape of NPs were analysed by the scanning electron microscope (SEM, FEI QUANTA 250 FEG). Dissolved NPs were diluted 50 times with distilled water from their dissolved NP solutions. 5 μL solutions were dropped on an aluminum foil and samples were left for the drying for one day. Then, dried samples were coated with gold using EMITECH K550X in a vacuum for SEM imagining. The accelerating voltages were 5–7 kV. Also, size measurements of NPs were analysed by using a Malvern dynamic light scattering (DLS) at a wavelenght of 632 nm. The scattering angle was set at 173°. The zeta potential of nanoparticles were determined by a Malvern dynamic light scattering (DLS) Nano-ZS instrument (Worcestershire, UK).

2.4. Preparation of salicylic acid (SA) loaded cBSA NPs and BSA NPs

62.5 mg/mL cBSA (or BSA) was dissolved in distilled water and stirred for 20 min. Salicylic acid (SA) stock solutions were prepared in DMSO. Then, dissolved SA was added to the albumin solutions at different molar ratios SA:cBSA (or SA:BSA) 3:1, 5:1, 10:1, 25:1, 35:1 while keeping the DMSO content constant at less than 2% (v/v). The mixtures were incubated for 30 min with 750 rpm stirring. After the incubation, acetonitrile was added dropwise by using syringe pump with a flow rate of 1 mL/min. The volume ratio of acetonitrile and water was adjusted to 4:1. 18 μL of 8% (v/v) cross-linking agent glutaraldeyhde was added. The reaction was stirred with a magnetic stirrer overnight at 750 rpm.

2.5. Measuring the percentages of entrapment efficiency and drug loading

The SA loaded cBSA NPs and BSA NPs were centrifuged at 14,000 rpm for 45 min. Pellets of NPs were lyophilized, and supernatants were collected and analysed by the UV–visible spectrophotometer to calculate the percentage of drug entrapment efficiency (Eq. (1)) and the percentage of drug loading (Eq. (2)). Supernatants were diluted with acetonitrile:water (4:1, v/v) to measure the concentration of SA in the supernatants by using LAMBDA 365 UV–visible spectrophotometer (PerkinElmer). For the calibration curve, salicylic acid stock solutions in the acetonitrile:water (4:1, v/v) were prepared. The curve was linear and passed through the origin ($R^2 = 0.9988$, $n = 5$).

$$Entrapment\ Efficiency\ (\%) = \frac{Initial\ drug\ weight - Drug\ weight\ in\ supernatant}{Initial\ drug\ weight} X\ 100 \quad (1)$$

$$Drug\ Loading(\%) = \frac{Weight\ of\ drug\ in\ nanoparticles}{Total\ weight\ of\ nanoparticles} X100 \quad (2)$$

Lyophilized drug loaded NPs were diluted in distilled water and washed 2 cycles with distilled water for the size and zeta potential measurements by dynamic light scattering (DLS). The size and morphology of drug loaded nanoparticles were characterized by using scanning electron microscope (SEM).

2.6. In vitro release of SA from cBSA NPs and BSA NPs

In vitro release of SA from NPs prepared with SA:cBSA and SA:BSA molar ratios 35:1 were perfomed in phosphate buffer (0.1 M, pH 7.4). 6 mg SA-cBSA NPs and 10 mg SA-BSA NPs containing the same amount of SA were dispersed in 2 mL of distilled water and 1 mL of phosphate buffer. Then the solutions were transferred in 3 mL D-tube dialyzers (Merck, MWCO 6–8 kDa). The dialyzer tube was placed in a beaker containing 150 mL phosphate buffer at 37.5 °C under stirring at 200 rpm. At predetermined time points, 2 mL of sample was collected and measured by UV–visible spectrophotometer to determine the released amount of SA from cBSA NPs and BSA NPs. After measurements, the 2 mL of samples were put back in the beakers.

2.7. Cell uptake and imaging

Huh-7 cells were cultured at 37 °C incubator with 5% CO_2 in DMEM. DMEM was prepared with 1% penicillin/streptomycin and 10% FBS. First, 500,000 Huh-7 cells were washed with PBS and labeled with 2.5 μL DiI in 47.5 μL PBS at 37 °C for 20 min. Cells were washed once with 10% FBS in PBS, twice with PBS and suspended in complete DMEM. Then 50,000 cell/chamber were seeded in 8-well chamber slide (SPL), grown overnight before treatment with NPs. Cells were treated with 0.1 mg/mL, 0.05 mg/mL, 0.01 mg/mL and 0.001 mg/mL FITC-cBSA NPs or FITC-BSA NPs in fresh DMEM and incubated 24 h at 37 °C. Then, cells were washed with PBS and fixed with 4% PFA for 20 min. Finally, the nuclei were stained with 4 mg/mL DAPI for 5 min and 8-well chamber slides were covered with a drop of glycerol, before closing with coverslips. Slides were imaged with Confocal Microscope (Zeiss LSM880) using 20X and 63X objectives. Z-stacks were taken 3 μm apart in 63X. Images were processed with Image J to generate overlay images. Same laser and scanning settings were used for each image.

2.8. Cell viability assay

Cell viability was assessed with CCK-8 assay as follows: Huh-7 cells were seeded 7,000 cell/well in 96-well plates incubated in DMEM with 10% FBS at 37 °C with 5% CO_2 incubator. 10 mg/mL cBSA NP (and BSA NP) suspensions were prepared in DMEM, and cells were treated with serial dilutions of NPs at final concentrations of 4 mg/mL - 0.05 mg/mL. After 24 h incubation with NPs, cell medium was replaced with fresh DMEM containing 10 μL CCK-8 reagent (Abcam 228554), incubated at 37 °C for 3 h. Absorbance at 460 nm was measured with Thermo Fisher Multiskan Go at the beginning and end of 3 h incubation. The increase in signal was used for calculating relative cell survival compared to control wells with 100% survival. Each measurement was done in 3 replicas, and % viability was calculated.

3. Results and discussion

3.1. Synthesis and characterization of cBSA protein

Cationized BSA (cBSA) was obtained by ammination of the surface with ethylenediamine through an amide linkage. Addition of ethylenediamine to the carboxylic acid groups of amino acids including aspartic acids (Asp) and glutamic acids (Glu) were detected by the MALDI TOF mass spectrum (Fig. 1 (A)). Increase in the average molecular weight of BSA from 66490 g/mol to 68545 g/mol indicated that on average 49 ethylenediamine molecules reacted with the available carboxylic acid side chains of 99 amino acids (Asp and Glu). ATR-FTIR spectroscopy also showed the cationization of BSA with ethylenediamine (Fig. 1 (B)). The band at 1400 cm^{-1} was attributed to the C═O bond in the side chain carboxylic groups of Asp and Glu in BSA. Conjugation of ethylenediamine with Asp and Glu decreased the signal intensity at this wavenumber, indicating the decrease of carboxyl group in cBSA [41]. Consequently, the negative net charge on the BSA (-11 ± 1) was converted into a positive net charge ($+25 \pm 2$) at pH 7.0 (Fig. 1 (C)). Also, the zeta potentials of BSA and cBSA at different pH values (3.0–12.0) were measured (Fig. 1 (C)). For BSA, the positive zeta potential decreased from +20 to 0 when pH was raised from 3.0 to 5.0. Above the isoelectric point (pI = 5.0), the zeta potential of BSA decreased with increasing the pH. On the other hand, the pI value of the cBSA was determined as about 10.1. Thus, a net positive charge on cBSA is maintained over a broad pH range.

3.2. Synthesis and characterization of cBSA NPs and BSA NPs

Here, cationic BSA nanoparticles (cBSA NPs) were prepared by a simple desolvation process at pH 7.0. Different desolvating agents such as methanol, ethanol, propanol, isopropanol, acetone and acetonitrile

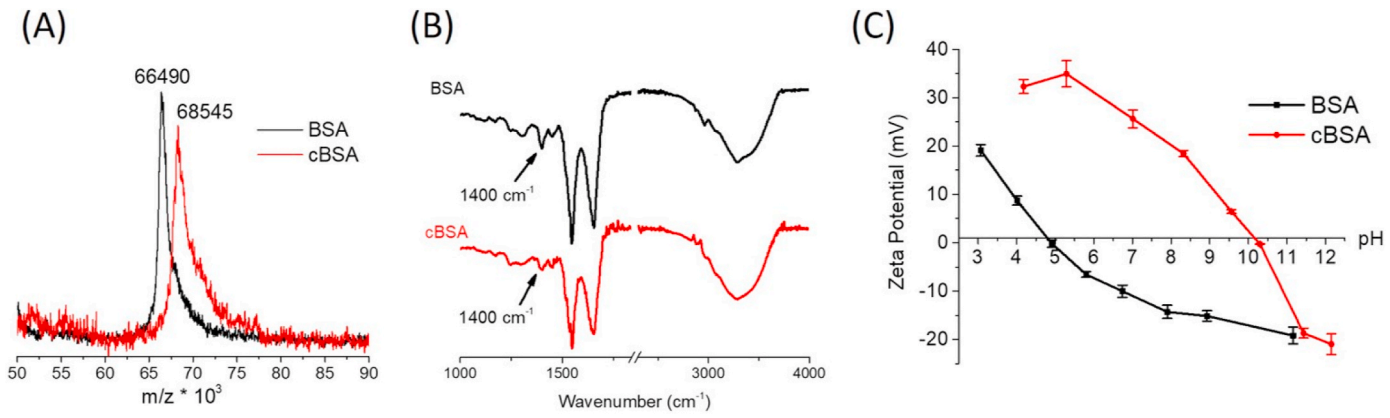

Fig. 1. (A) MALDI-TOF mass spectra of native BSA (black) and cationic BSA (cBSA) (red) proteins. (B) ATR-FTIR spectra of native BSA (black) and cBSA aqueous solutions (red). (C) The zeta potentials of native BSA (black) and cationic BSA (cBSA) (red) proteins at different pH values from 3.0 to 12.0. (For interpretation of the references to colour in this figure legend, the reader is referred to the Web version of this article.)

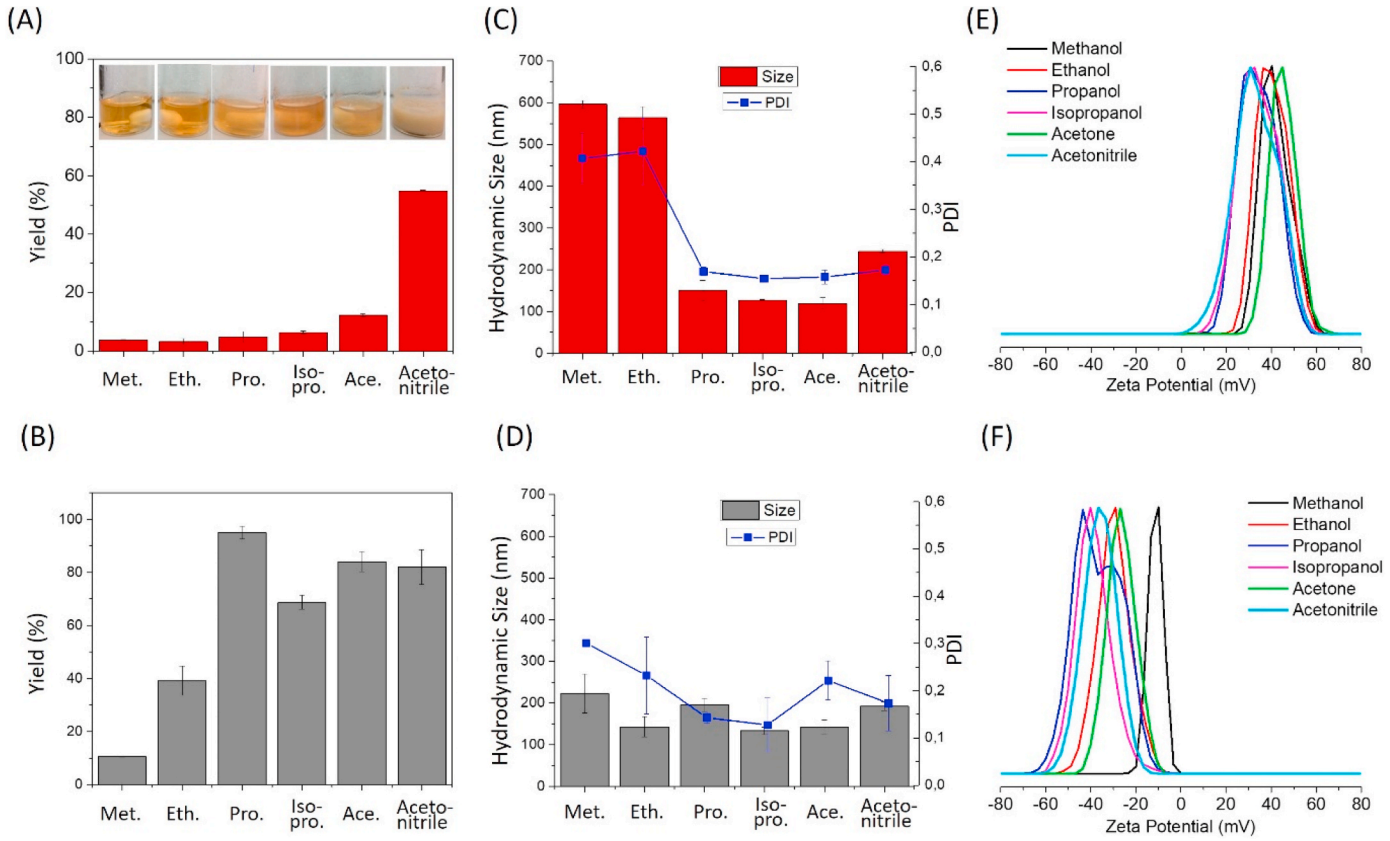

Fig. 2. The yield percentages of cBSA (A) and BSA (B) NPs formations, the average hydrodynamic sizes and PDI values of cBSA (C) and BSA (D) NPs, and the zeta potentials of (E) cBSA and (F) BSA NPs produced with different desolvating agents including methanol, ethanol, propanol, isopropanol, acetone and acetonitrile. Experiments were performed in triplicate.

were used to produce cBSA NPs. Fig. 2 (A) shows the yield % of cBSA NPs formation when 62.5 mg of cBSA dissolved in 1 mL of water. Using alcohols e.g. methanol, ethanol, propanol or isopropanol as desolvating agents produced very low amounts of cBSA NPs with the average yield % of NP formations 3.7 ± 0.1%, 3.2 ± 1.1%, 4.7 ± 1.9% and 6.3 ± 0.4%, respectively. These results showed that alcohols with short carbon chains have poor desolvation ability for cationic BSA. Increasing the length of alkyl chain of alcohol from one to three slightly improved the yield of cBSA NP formation. Acetone and acetonitrile are polar aprotic solvents which are capable of forming hydrogen bonds with only hydrogen donors. Addition of acetone to cBSA solution produced cBSA NPs with 12.2 ± 0.6% yield of NP formation which was relatively higher than the results of used alcohols. On the other hand, using acetonitrile as desolvating agent produced a significant amount of cBSA NPs with 54.8 ± 0.2% yield of NP formation. Higher dipole moments of acetonitrile (μ = 4.00) and also acetone (μ = 2.90) could favor the cationic albumin binding compared to the used alcohols with lower dipole moments; methanol (μ = 1.70), ethanol (μ = 1.70), propanol (μ = 1.60), isopropanol (μ = 1.63) [42,43]. Therefore, extensive electrostatic interaction between acetonitrile and cBSA, together with the hydrophobic interactions and hydrogen bonding led to more cBSA NPs formation.

On the other hand, when non-modified BSA was used to produce

NPs, all used desolvation agents yielded significant amount of NPs, except for methanol with 10.5 ± 0.2% yield of NP formation (Fig. 2 (B)). Methanol with the lowest carbon chain has a low desolvation ability for the native BSA, too. Addition of ethanol, propanol, isopropanol, acetone or acetonitrile to an aqueous solution of BSA produced considerable amount of BSA NPs with 39.1 ± 5.5%, 95 ± 2.4%, 68.6 ± 2.6%, 84.0 ± 3.7% and 82.0 ± 6.5% yields of NP formations, respectively. Increasing the length of carbon chain in the used alcohols induced more BSA desolvation due to the larger hydrophobic interactions between BSA and the alcohols [28]. Addition of acetone or acetonitrile enabled production of significant amounts of BSA NPs, in accord with literature findings [44,45].

Acetonitrile-albumin interaction could be analysed with fluorescence spectroscopy since albumin possess intrinsic tryptophan (Trp) fluorescence (Trp-212 and Trp-134). Fig. S1 showed the fluorescence emission spectra of BSA and cBSA aqueous solutions with different doses of acetonitrile. Addition of acetonitrile to the BSA solution shifted the fluorescence emission peak from 348 nm to 339 nm (Fig. S1 (A, C)). This blue shift indicates that the environmental hydrophobicity of the Trp increased upon addition of acetonitrile. The signal intensity is also very sensitive to the microenvironment of Trp. At low acetonitrile content (10% (v/v)), Trp was wrapped tightly inside the protein which reduces the energy loss and fluorescence quenching [46]. As a result, the signal intensity increased. Addition of 20% and 30% (v/v) acetonitrile deformed BSA more. This leads to more Trp exposed to water which decreases its fluorescence intensity. Above 30% (v/v) of acetonitrile, aggregation of BSA reduced the Trp exposure to water, and so increased its fluorescence intensity [47]. On the other hand, the fluorescence peak of cBSA was observed at 340 nm (Fig. S1 (B, D)). Cationization of BSA with ethylenediamine shifted the fluorescence peak from 348 nm to 340 nm. This blue shift indicated that the hydrophobicity of the system increased with ethylenediamine conjugation. The fluorescence peak position of cBSA was unchanged upon addition of acetonitrile up to 80% (v/v). This shows that the environmental hydrophobicity of the Trp in cBSA did not change remarkably upon addition of acetonitrile. Also the signal intensity of cBSA increased gradually with increasing acetonitrile content due to the changes in the microenvironment of Trp. Addition of acetonitrile induced cBSA aggregation which increased its fluorescence intensity [47].

Fig. 2(C) and (D) show the average hydrodynamic sizes of produced cBSA NPs and non-modified BSA NPs using different desolvating agents and the corresponding PDI values, respectively. A limited number of cBSA NPs obtained with methanol and ethanol were analysed with DLS and SEM techniques (Figs. 2 (C) and Fig. 3 (A)). When methanol or ethanol were used, the obtained average hydrodynamic sizes were about 600 nm with the corresponding PDI values of about 0.45. This PDI value showed the presence of cBSA NPs with a wide range of particle sizes. Actually, their SEM images showed the formation of cBSA NPs aggregates (Fig. 3 (A) and (B)). On the other hand, using propanol, isopropanol or acetone yielded smaller nanoparticles with average hydrodynamic sizes about 150 ± 24, 127 ± 1 and 119 ± 13 nm, respectively. Their PDI values which were lower than 0.2 showed the presence of cBSA NPs with a relatively uniform size distribution. Addition of acetonitrile to cBSA aqueous solution produced relatively larger cBSA NPs with average hydrodynamic size 244 ± 4 nm compared to the those of cBSA nanoparticles after addition of propanol, isopropanol or acetone. Also, the corresponding PDI value was about 0.2 indicating a narrow size distribution. Fig. 3 (C-E) showed the SEM images of well dispersed spherical cBSA NPs obtained with use of propanol, isopropanol, acetone and acetonitrile. The sizes of cBSA NPs obtained from SEM images smaller than the results of DLS because of dry state.

On the other hand, the hydrodynamic sizes of non-modified BSA NPs produced using different desolvating agents were very similar to each other (Fig. 2 (D)). Their average sizes varied between 100 and 200 nm. In addition, the SEM images showed well dispersed spherical BSA NPs with similar average particle sizes below 100 nm (Fig. 4). Obtaining higher average particle size by DLS due to the formation of hydration shell and swelling of nanoparticles with water.

The synthesized cBSA NPs and BSA NPs had also different zeta potentials. The zeta potentials of the produced cBSA NPs with different desolvation agents were found to be between +38 and + 44 mV (Fig. 2 (E)). On the other hand, native BSA NPs obtained from non-modified BSA using different desolvation agents had negative potential charges between −43 and −27 mV. Only, BSA NPs produced after addition of

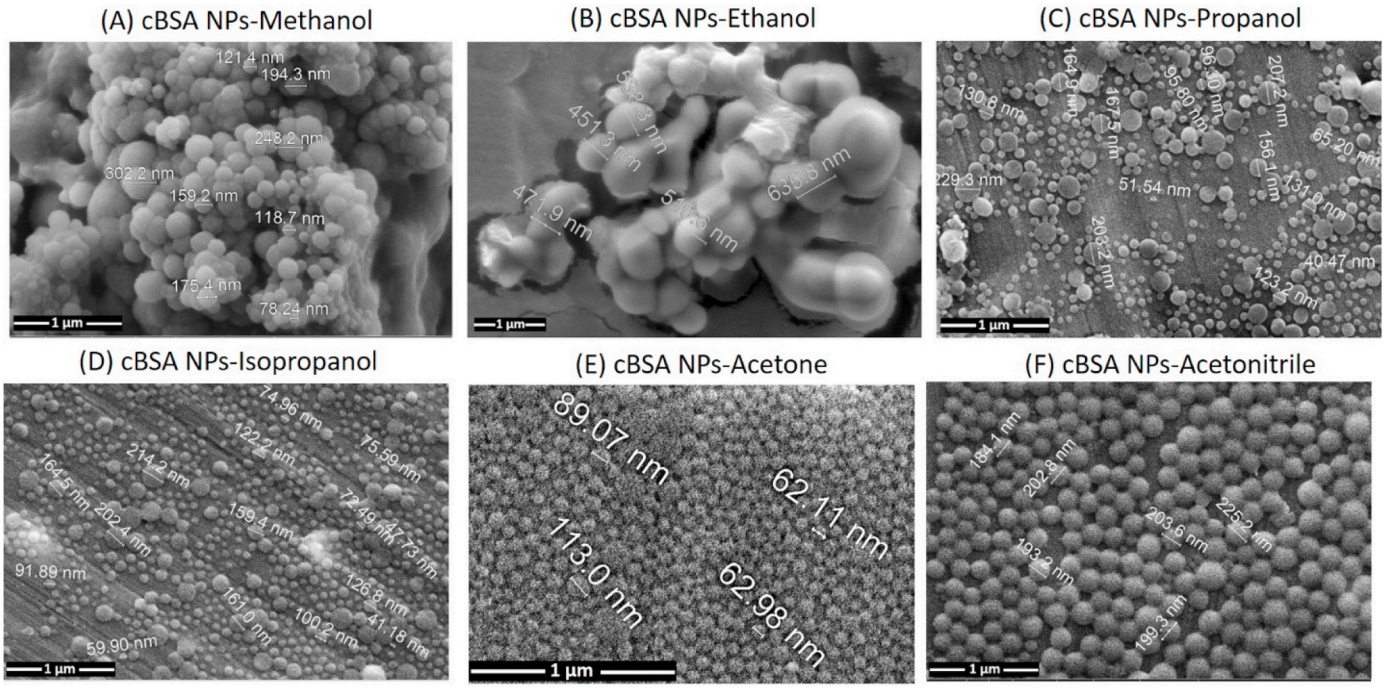

Fig. 3. SEM images of cBSA NPs produced using different desolvating agents; (A) methanol, (B) ethanol, (C) propanol, (D) isopropanol, (E) acetone and (F) acetonitrile.

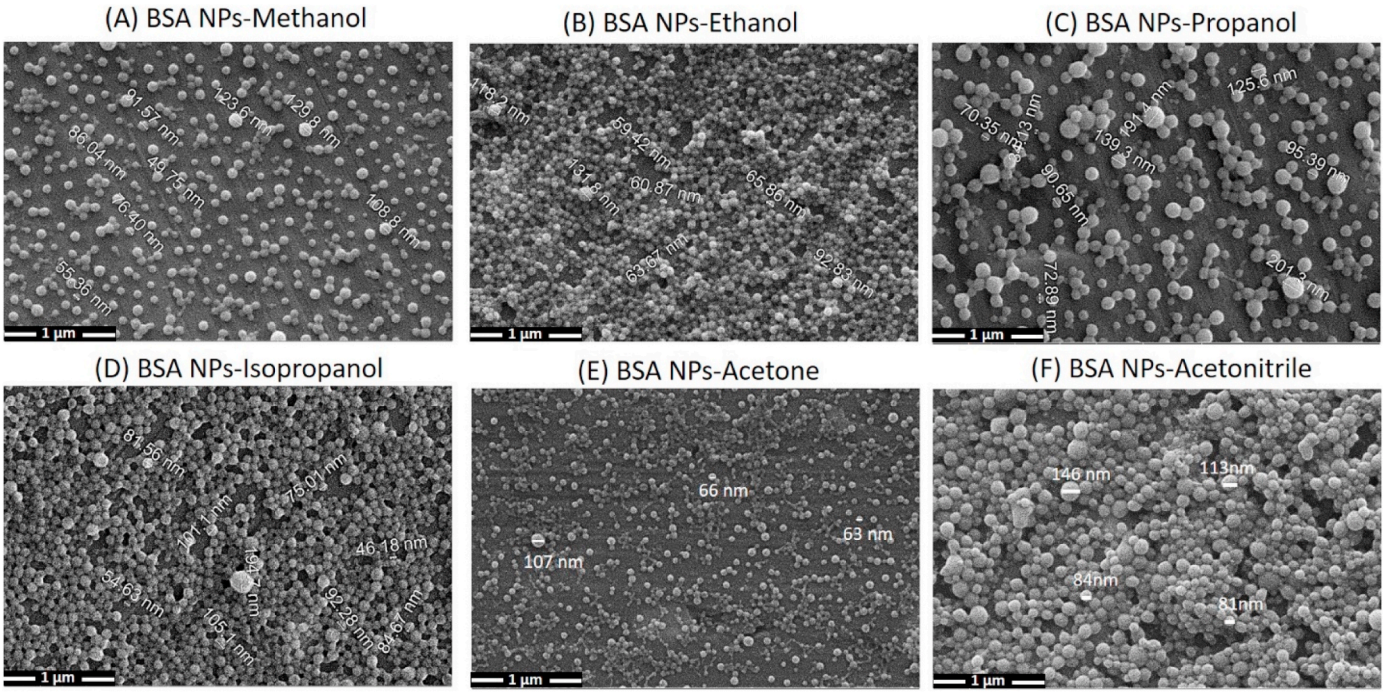

Fig. 4. SEM images of BSA NPs produced using different desolvating agents; (A) methanol, (B) ethanol, (C) propanol, (D) isopropanol, (E) acetone and (F) acetonitrile.

methanol had a lower net negative charge of −11 mV (Fig. 2 (F)).

3.3. Drug loading and release properties of cBSA NPs and BSA NPs

Herein, cBSA NPs fabricated by acetonitrile precipitation was used in order to study the drug loading and release properties, and also to study cell uptake and toxicity. Acetonitrile was chosen due to high yield when compared to other tested desolvating agents (Fig. 2(A)). According to SEM analysis, the NP size is ~200 nm (Fig. 3 (E)), small enough for the cellular uptake. For comparison, drug loaded non-modified BSA NPs were also prepared by addition of acetonitrile.

Salicylic acid (SA) loaded cBSA NPs and BSA NPs were prepared by the incorporation method. The water solubility of SA is very low therefore concentrated SA solutions prepared in DMSO were incorporated at the time of NPs preparation. SA entrapment efficiency (wt%) into cBSA NPs and BSA NPs were shown in Fig. 5 (A). At low SA:cBSA molar ratios e.g. 3:1 and 5:1, the SA entrapment efficiency was determined as 55 wt%. Increasing the SA:cBSA molar ratios to 10:1, 25:1 and 35:1 decreased the SA entrapment efficiencies to 45, 37 and 37 wt%, respectively. Also, drug loading results of cBSA NPs were shown in Fig. 5 (B). SA content in the cBSA NPs increased with increasing the initial SA:cBSA molar ratio and reached to 5.6 wt% at a molar ratio 35:1. Maximum 35:1 (SA:cBSA) molar ratio was used due to the solubility restriction of SA in aqueous medium.

On the other hand, SA loading into the native BSA NPs without cationization was not possible at SA:BSA molar ratios 3:1 and 5:1 (Fig. 5 (A), black). However, at higher molar ratios of SA to BSA 10:1, 25:1 and 35:1, the SA entrapment efficiencies were determined as 6, 37 and 40 wt %, respectively. Also, drug loading results of BSA NPs were found as 0.2, 2.1 and 3.0 wt% when 10:1, 25:1 and 35:1 (SA:BSA) molar ratios were used, respectively (Fig. 5 (B), black). Obtaining SA entrapment in the native BSA NPs only at higher SA:BSA molar ratios can be explained by

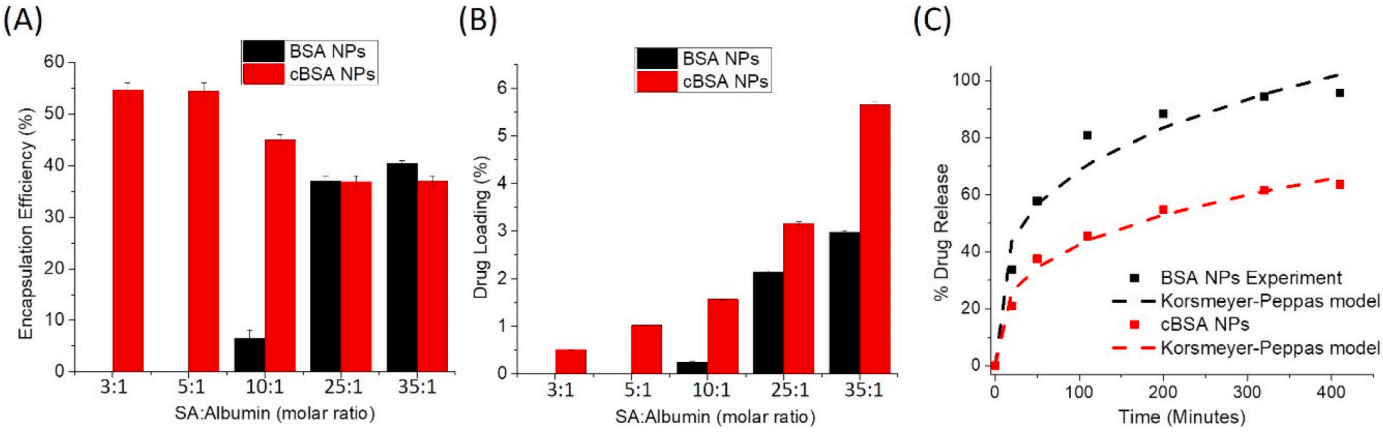

Fig. 5. (A) Salicylic acid (SA) entrapment efficiency (wt%) results and (B) SA loading (wt%) results of cBSA NPs (red) and BSA NPs(black) with respect to the initial molar ratio of SA:Albumin. (C) The cumulative percentages of SA released from the cBSA NPs (red) and BSA NPs (black) prepared with the 35:1 (SA:Albumin) molar ratio with Korsmeyer-Peppas fitting model. Experiments were performed in triplicate. (For interpretation of the references to colour in this figure legend, the reader is referred to the Web version of this article.)

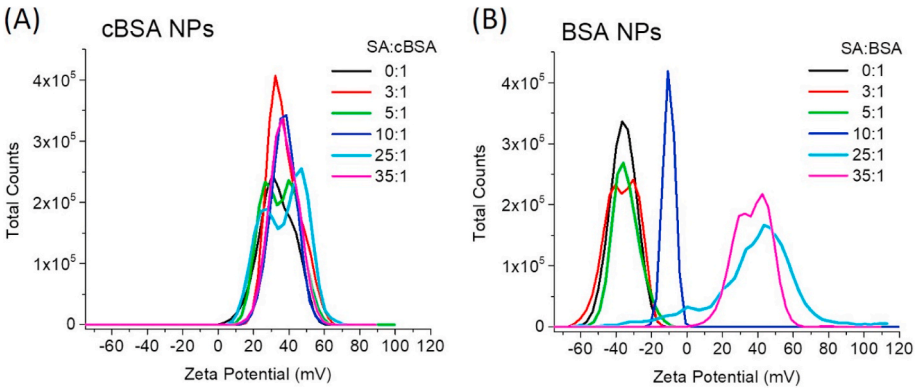

Fig. 6. The zeta potentials of (A) SA loaded cBSA NPs and (B) SA loaded BSA NPs produced with different SA:cBSA and SA:BSA molar ratios, respectively. Nanoparticles were prepared using acetonitrile.

the cationization of BSA due to the high SA content in the medium. Addition of high SA content into the BSA aqueous solution decreased the pH value of BSA solution. The measured pH values of BSA solutions after addition of SA with the ratios of 10:1, 25:1 and 35:1 (SA:BSA) were 6.1, 5.0 and 4.6, respectively. At acidic pH, the surface charge of BSA protein became cationic (without ethylenediamine conjugation). As a result, similar to the zeta potentials of SA loaded cBSA NPs +40 mV (Fig. 6 (A)), non-modified BSA NPs gained positive net charges +37.5 and + 36.9 mV in the presence of high levels of SA, 25:1 and 35:1 (SA:BSA), respectively (Fig. 6 (B)). At 10:1 (SA:BSA) molar ratio, the obtained BSA NPs had a lower net negative charge about −10 mV compared to the zeta potentials of BSA NPs −36 mV when 0:1, 3:1 and 5:1 (SA:BSA) molar ratios were used (Fig. 6(B)). Consequently, non-modified BSA NPs could only load the SA significantly when high levels of SA (25:1 and 35:1, SA:BSA) were incorporated.

Also, loading of SA in the cBSA NPs and BSA NPs affect the sizes of nanoparticles differently. Fig. 7 shows the SEM images of drug loaded cBSA NPs and BSA NPs at different SA:Albumin ratios, 0:1, 25:1 and 35:1. Loading of SA in the cBSA NPs with 25:1 and 35:1 SA:cBSA molar ratios decreased the sizes of cBSA NPs, gradually. Before SA loading, the average size of cBSA NPs was around 200 nm. However, after SA loading, it decreased to around 100 nm (Fig. 7, top). Addition of high numbers of SA (25:1 and 35:1, SA:cBSA) into the cBSA protein solution decreased the pH value of the protein solution to 5 which makes the cBSA proteins more cationic (Fig. 1 (C)). Therefore, higher electrostatic repulsive forces limited the number of cBSA proteins involved in aggregation process which causes smaller particle formation. The DLS results were also consistent with the SEM results. The average hydrodynamic sizes decreased from 244 nm (PDI: 0.2) to 182 nm (PDI: 0.22) and 170 nm (PDI: 0.21) after SA loadings (25:1 and 35:1, SA:cBSA), respectively.

Conversely, for native BSA NPs, drug loading first increased the average size of SA loaded BSA NPs enormously at 25:1 SA:BSA ratio, and then decreased it at 35:1 SA:BSA ratio (Fig. 7, bottom). Yet, at 35:1 SA:BSA molar ratio the final average size of SA-BSA NPs (~275 nm) was much larger than that of bare BSA NPs (~100 nm). This might be explained with the effect of SA on the surface charge of BSA protein in solution. Addition of SA to BSA solution at 25:1 and 35:1 M ratios (SA:BSA) decreased the pH of the solution to 5.0 and 4.6, respectively. In Fig. 1 (C), the isoelectric point of BSA was found as 5.0. Therefore, at

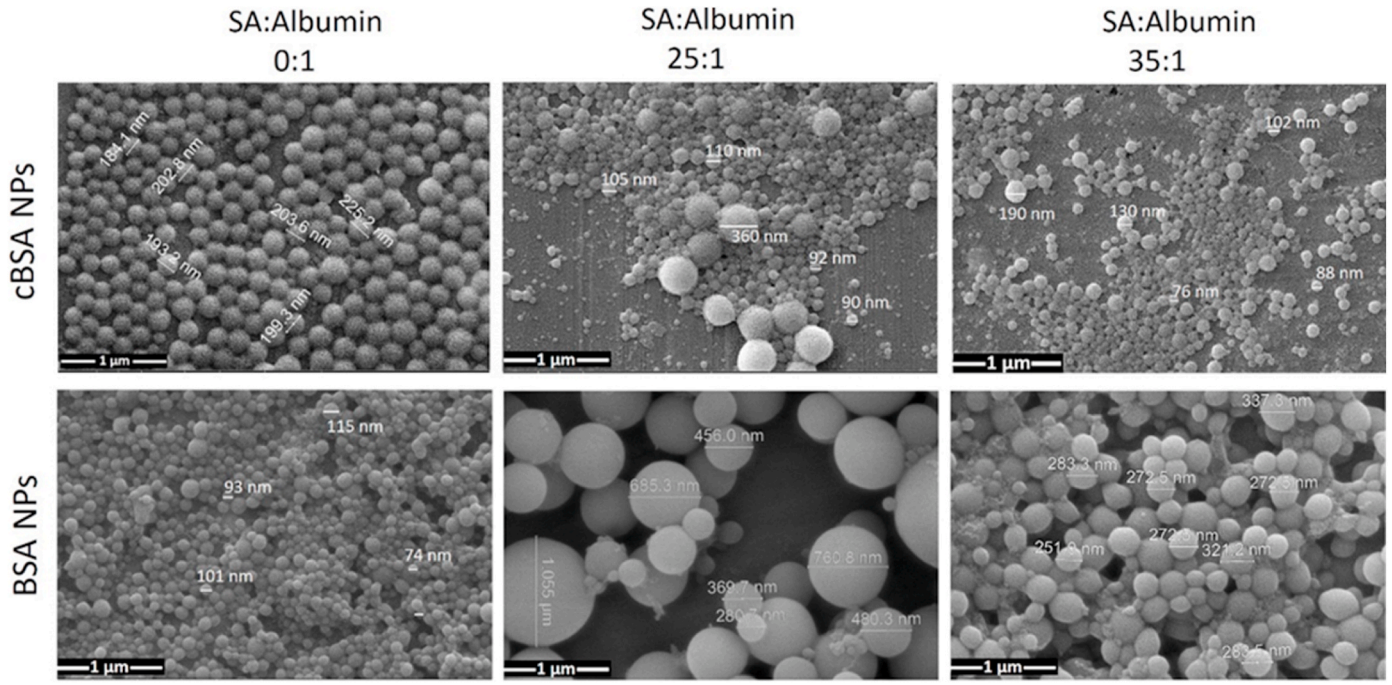

Fig. 7. SEM images of cBSA NPs (top, left) and BSA NPs (bottom, left) without SA loading. Drug loaded cBSA NPs (top) and BSA NPs (bottom) obtained with mixtures of 25:1 (middle) and 35:1 (right) SA:Albumin molar ratios.

25:1 M ratio (SA:BSA), the pH of BSA solution reached to the isoelectric point.

Keeping the zeta potential of BSA around the isoelectric point favors protein-protein hydrophobic interactions which induce much larger particle formation (Fig. 7, bottom-middle). However, addition of more SA into BSA solution with 35:1 M ratio decreased the pH value of solution to 4.6 which makes the BSA cationic. Therefore, this positive surface charge on the BSA proteins relatively inhibited the formation of larger BSA NPs but still larger than the bare BSA NPs (Fig. 7, bottom-right). Their average hydrodynamic sizes were also supported their SEM results. The average sizes of BSA NPs (193 nm, PDI: 0.17) increased to 735 nm (PDI: 0.284) and 268 nm (PDI:0.10) at 25:1 and 35:1 M ratios (SA:BSA), respectively.

In vitro release of SA from the SA loaded cBSA NPs prepared with the 35:1 (SA:cBSA) molar ratio was investigated at 37 °C in 0.1 M phosphate buffer, pH 7.4 (Fig. 5 (C)). 6 mg of SA-cBSA NPs dispersed in 3 mL water/phosphate buffer (2:1, v:v) was placed in a D-tube dialyzer, and then the tube was put into a beaker containing 150 mL of phosphate buffer (pH 7.4).The total release of SA from cBSA NPs at the end of 53 h was found to be 78% (Fig. S2 (A)). The SA release profile of cBSA NPs was indicative of a biphasic pattern. An initial burst release within 50 min corresponding to the 37% of loaded SA was followed by a relatively slower release of SA. In order to compare the SA release profile of cBSA NPs with that of non-modified BSA NPs, 10 mg of SA-BSA NPs containing the same amount of SA were used. Again, the SA-BSA NPs were prepared with the 35:1 (SA:BSA) molar ratio. Fig. 5 (C) shows an initial burst of SA release within 50 min, during which up to 58% of loaded drugs are released from the non-modified BSA NPs. At the end of 7 h, the total SA release from BSA NPs was found to be around 100%.

Also, the drug release mechanism of cBSA NPs was studied by mathematical methods. The drug release data were treated according to Korsmeyer-Peppas model (cumulative % drug release vs. n power of time) and Higuchi model (cumulative % drug release vs. square root of time) [48]. Fitting models of SA release from BSA NPs and cBSA NPs were shown in Fig. 5 (C) and Fig. S2 (B). The SA release process followed Korsmeyer-Peppas model for both BSA NPs and cBSA NPs with the higher correlation (R^2) values of 0.98 and 0.99, respectively (Fig. 5 (C)). On the other hand, the obtained R^2 values of Higuchi models are 0.94 and 0.97 for BSA NPs and cBSA NPs, respectively (Fig. S2 (B)). The release power (n) value obtained from the Korsmeyer-Peppas model also indicates the mechanism of drug release from the carrier. For spherical carriers, values of n less than 0.43 indicate that the drug release mechanism follows Fickian diffusion mechanism [49]. Here, the n values obtained using Korsmeyer-Peppas models are 0.28 and 0.30 for BSA NPs and cBSA NPs, respectively, which suggest that the release of SA from both NPs is controlled by Fickian diffusion. In addition, the SA release rate constants (k) obtained from the Korsmeyer-Peppas model are 19 and 10 for BSA NPs and cBSA NPs, respectively, which indicate the slower release rate of SA from cBSA NPs. The drug release from non-modified BSA NPs is much faster than that from cBSA NPs. Since non-modified BSA gains positive charge after addition of SA, the NP zeta potential gradually became negative again with releasing SA. After complete drug release, the zeta potential of non-modified BSA NPs was found to be −39 mV. However, zeta potential of cBSA NPs did not depend on the presence of SA so much. Therefore, durable electrostatic interaction between cBSA and SA retards the drug release.

3.4. Cellular uptake and toxicity of cBSA NPs and BSA NPs

Cellular uptake and toxicity of cBSA NPs and BSA NPs were investigated in cancer cell line, Huh7. Fluorescein isothiocyanate (FITC) labeled cBSA and BSA were used to visualize the distribution in cells.

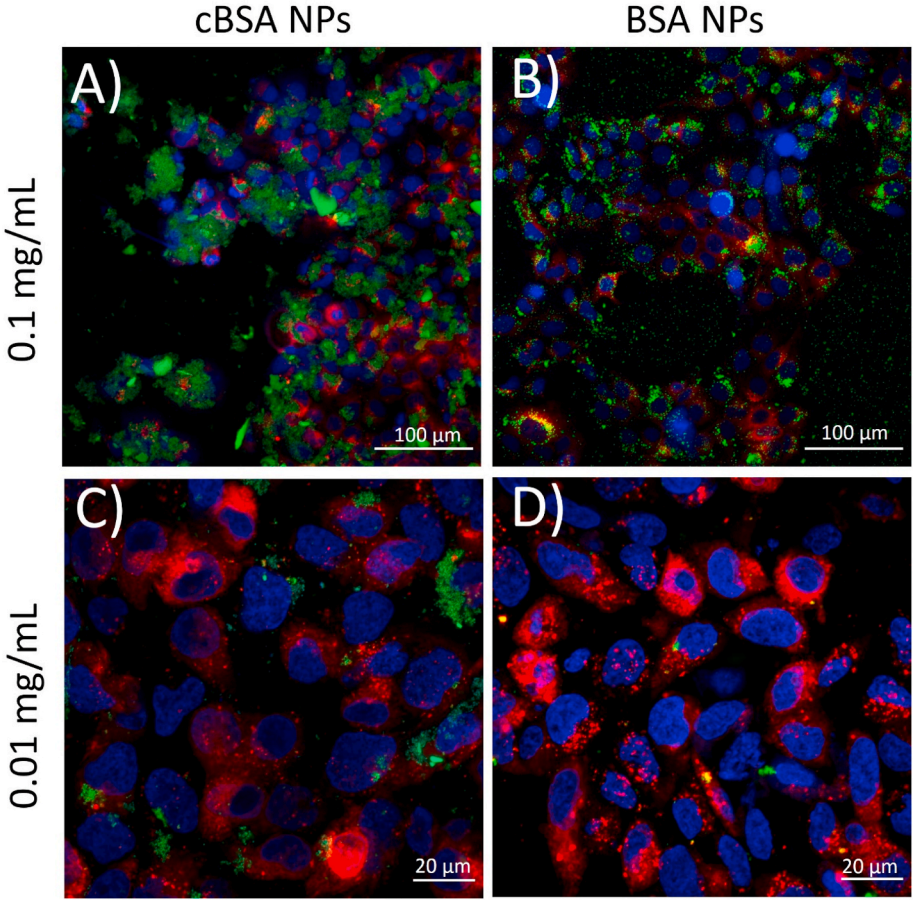

Fig. 8. The cellular uptake of cBSA NPs (A, C) and BSA NPs (B, D) with 0.1 mg/mL and 0.01 mg/mL, respectively. Huh 7 cells were treated 24 h with NPs that were prepared using FITC labeled cBSA and BSA. Cell membranes were stained with DiI (red) and nuclei were stained with DAPI (blue). Images were recorded at confocal microscope with 20X (A, B) or 63X Oil (C, D) objective. Scale bar = 100 µm (A, B) and = 20 µm (C, D). (For interpretation of the references to colour in this figure legend, the reader is referred to the Web version of this article.)

First, cells were incubated with 0.1 mg/mL cBSA NP or BSA NP for 24 h. Both non-modified and cationic NPs entered the cells, however the number of NP per cell was extremely high for cBSA NP compared to BSA NP (Fig. 8 (A), (B)). cBSA NPs appeared to accumulate in large numbers in the cells, as expected due to increased electrostatic attraction. Next, we treated cells with a low concentration (0.01 mg/mL) of NPs to further demonstrate the effect of cationic surface charge. At 0.01 mg/ml the cellular uptake of BSA NPs was close to none, with very few cells containing few NPs. On the other hand, cBSA NPs were still efficiently taken by cells and several NPs per cell were detected (Fig. 8 (C), (D)). These data show that at both NP concentrations, the uptake amounts of cBSA NPs were much higher than that of non-modified BSA NPs. The significant difference between the cellular uptake of cBSA NPs and that of non-modified BSA NPs is due to electrostatic interactions between cBSA and negatively charged cell membrane. Supporting this, several studies have shown that cationic NPs demonstrate better adherence to the cell membrane which causes higher intracellular accumulation compared to the negatively and neutrally charged NPs [35,36,50].

The cytotoxic effect of cBSA NPs at various concentrations were measured with CCK8 viability assay in HuH7 cells, and cytotoxicity of cBSA NPs was found to be concentration dependent. After 24 h, the cell viability was not affected when treated with 0.05–0.2 mg/mL of cBSA NP concentrations. cBSA NP concentration between 0.2 and 1.0 mg/ml caused gradual decrease in viability. From Fig. 9 (red), it can be derived that the half maximal effective concentration (EC_{50}) of cBSA NPs was 0.8 mg/mL. Above 1.0 mg/mL, however 40% viable cell population was not affected significantly from increased cBSA NP concentration since the saturation of uptake was achieved already. On the other hand, cellular uptake of non-modified BSA NPs had no significant influence on the cell viability up to 4 mg/mL concentrations for 24 h (Fig. 9, black). cBSA NPs caused a pronounced cytotoxicity compared to the native BSA NPs. This could be explained by the strong adherence of cBSA NPs to cell membrane which may cause cell membrane integrity disruption, and/or mitochondrial and lysosomal damage with consequent production of reactive oxygen species (ROS) [50]. However, the cell viability up to 0.1 mg/mL cBSA NPs was still around 100% in spite of a significant accumulated amount of cBSA NPs in the cells (Fig. 8 (A)). The cell uptake measurements clearly showed that 0.1 mg/mL cBSA NPs strongly accumulated in the cell without causing any toxic effect.

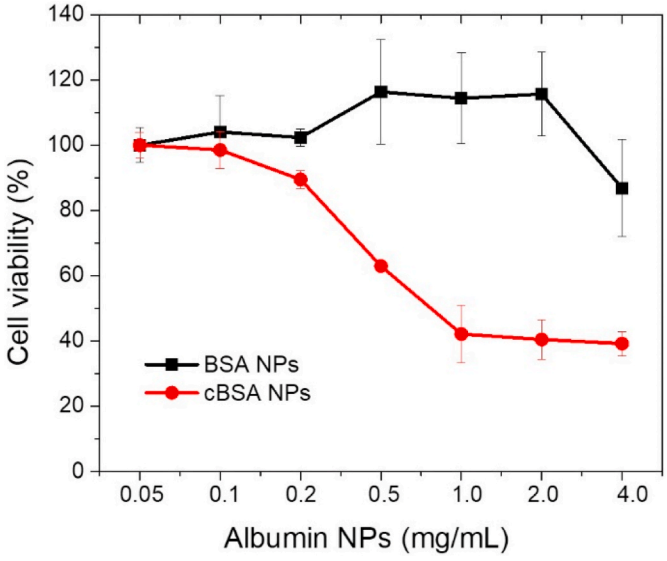

Fig. 9. Cell viability of cBSA NPs (red) and BSA NPs (black). The cells were incubated with different concentrations of NPs: 0.05, 0.1, 0.2, 0.5, 1.0, 2.0 and 4.0 mg/mL for 24 h incubation times. Experiments were performed in triplicate. (For interpretation of the references to colour in this figure legend, the reader is referred to the Web version of this article.)

4. Conclusion

To sum up, we fabricated cBSA NPs using a simple desolvation method, and then compared them with anionic native BSA NPs in terms of drug loading, drug release and cellular uptake. cBSA was obtained by ammination of the BSA surface with ethylenediamine, and was characterized by MALDI-TOF, ATR-FTIR and zeta potential measurements. cBSA NPs were obtained in a high formation yield (54.8%) only through addition of acetonitrile to the cBSA aqueous solution compared to the other desolvating agents such as methanol (3.7 wt%), ethanol (3.2 wt%), propanol (4.7 wt%), isopropanol (6.3 wt%) and acetone (12.2 wt%). Acetonitrile-BSA and acetonitrile-cBSA interactions were analysed with fluorescence spectroscopy. Addition of acetonitrile changed the environmental hydrophobicity of the Trp in BSA, but not changed that of the Trp in cBSA. Also the signal intensities of both BSA and cBSA increased gradually with increasing acetonitrile content due to the aggregation of albumins. Acetonitrile with the highest dipole moment interacts with cBSA proteins much electrostatically which caused more desolvation, in addition to the hydrophobic interaction and hydrogen bonding. The SEM analyses showed that the sizes of cBSA NPs and BSA NPs prepared using acetonitrile were around 200 nm and 100 nm, respectively.

Salicylic acid (SA) was used as a model drug to investigate drug loading and release properties of cBSA NPs which were prepared with acetonitrile. The reason for the choosing acetonitrile as a desolvating agent is that the yield % of cBSA NP formation is much higher when acetonitrile is used. SA was mixed with cBSA at different ratios throughout the desolvation process. At all used SA:cBSA molar ratios, SA was loaded in cBSA NPs with a maximum drug loading of 5.6 wt% (35:1). However, SA was not loaded in native anionic BSA NPs at low SA:BSA ratios. Yet, it was loaded at high SA:BSA ratios with a maximum drug loading of 3.0 wt% which was lower than that of cBSA NPs. This could be explained by decrease in the pH value of SA and BSA mixture at higher SA concentrations. Drug release properties of cBSA NPs and BSA NPs were also different. SA release behavior of cBSA NPs was slower than that of BSA NPs. For both BSA and cBSA NPs, the SA release process followed Korsmeyer-Peppas model with the high correlation (R^2) values of 0.98 and 0.99, respectively. In addition, SEM analyses showed that drug loading decreased the average sizes of cBSA NPs from 200 nm to 100 nm while drug loading increased the average sizes of BSA NPs from 100 nm to 275 nm. This is because the pH value of SA-BSA mixture became close to the isoelectric point of BSA which favors the BSA-BSA interactions.

Cationization of BSA markedly increased the cell uptake efficiency of BSA NPs. Electrostatic interactions between cBSA NPs and cell membrane resulted in preferential uptake into cells compared to that of anionic BSA NPs. Finally, the high level of cBSA NPs cellular accumulation decreased the cell viability significantly. The EC_{50} value of cBSA NPs was observed to be 0.8 mg/mL after incubation time of 24 h. Yet, the cell viability was around 100% up to 0.1 mg/mL of cBSA NPs treatment, with a significantly better cellular uptake compared to the uptake of BSA NPs.

CRediT authorship contribution statement

Tugce Ozmen Egesoy: Investigation, Methodology. **Merve Basol:** Investigation, Methodology. **Gulcin Cakan-Akdogan:** Supervision, Writing - review & editing, Formal analysis, Visualization. **Yasar Akdogan:** Conceptualization, Supervision, Writing - review & editing, Visualization, Project administration.

Declaration of competing interest

The authors declare that they have no known competing financial interests or personal relationships that could have appeared to influence the work reported in this paper.

Acknowledgment

This work was financially supported by Scientific and Technological Research Council of Turkey (TUBITAK) via 1002 Program under grant 119Z136. Authors thank Prof. Dr. Talat Yalçın for his help analyzing Maldi TOF Mass measurements. Authors thank IZTECH Center for Materials Research and Biotechnology and Bioengineering Research Center, National Mass Spectrometry Application and Research Center, and Izmir Biomedicine and Genome Center Optic Imaging Core Facility.

Appendix A. Supplementary data

Supplementary data to this article can be found online at https://doi.org/10.1016/j.jddst.2020.101931.

References

[1] D.C. Vimalson, S. Parimalakrishnan, N.S. Jeganathan, S. Anbazhagan, Techniques to enhance solubility of hydrophobic drugs: an overview, Asian J. Pharm. 10 (2016) 67–75.
[2] K.T. Savjani, A.K. Gajjar, J.K. Savjani, Drug solubility: importance and enhancement techniques, ISRN Pharm. (2012) 1–10, 2012.
[3] G. Zhou, X. Jin, P. Zhu, J. Yao, Y. Zhang, L. Teng, R.J. Lee, X. Zhang, W. Hong, Human serum albumin nanoparticles as a novel delivery system for Cabazitaxel, Anticancer Res. 36 (2016) 1649–1656.
[4] A.K. Jain, S. Thareja, In vitro and in vivo characterization of pharmaceutical nanocarriers used for drug delivery, Artif. Cells Nanomed, Biotechnol. 47 (2019) 524–539.
[5] M. Merodio, A. Arnedo, M.J. Renedo, J.M. Irache, Ganciclovir-loaded albumin nanoparticles: characterization and in vitro release properties, Eur. J. Pharmaceut. Sci. 12 (2001) 251–259.
[6] D. Zhao, X. Zhao, Y. Zu, J. Li, Y. Zhang, R. Jiang, Z. Zhang, Preparation, characterization, and in vitro targeted delivery of folate-decorated paclitaxel-loaded bovine serum albumin nanoparticles, Int. J. Nanomed. 5 (2010) 669–677.
[7] M.T. Larsen, M. Kuhlmann, M.L. Hvam, K.A. Howard, Albumin-based drug delivery: harnessing nature to cure disease, Mol. Cell. Ther. 4 (2016) 1–12.
[8] D. Sleep, J. Cameron, L.R. Evans, Albumin as a versatile platform for drug half-life extension, Biochim. Biophys. Acta 1830 (2013) 5526–5534.
[9] T. Peters, All about Albumin: Biochemistry, Genetics and Medical Applications, Academic Press, San Diego, 1995.
[10] K. Yamasaki, V.T. Chuang, T. Maruyama, M. Otagiri, Albumin–drug interaction and its clinical implication, Biochim. Biophys. Acta 1830 (2013) 5435–5443.
[11] M.A. Otagiri, Molecular functional study on the interactions of drugs with plasma proteins, Drug Metabol. Pharmacokinet. 20 (2005) 309–323.
[12] N. Desai, V. Trieu, Z. Yao, L. Louie, S. Ci, A. Yang, C. Tao, T. De, B. Beals, D. Dykes, P. Noker, R. Yao, E. Labao, M. Hawkins, P. Soon-Shiong, Increased antitumor activity, intratumor paclitaxel concentrations, and endothelial cell transport of cremophor-free, albumin-bound paclitaxel, ABI-007, compared with cremophor-based paclitaxel, Clin.Canc. Res. 12 (2006) 1317–1324.
[13] K. Komiya, T. Nakamura, C. Nakashima, K. Takahashi, H. Umeguchi, N. Watanabe, A. Sato, Y. Takeda, S. Kimura, N. Sueoka-Aragane, SPARC is a possible predictive marker for albumin-bound paclitaxel in non-small-cell lung cancer, OncoTargets Ther. 9 (2016) 6663–6668.
[14] M. Karimi, S. Bahrami, S.B. Ravari, P.S. Zangabad, H. Mirshekari, M. Bozorgomid, S. Shahreza, M. Sori, M.R. Hamblin, Albumin nanostructures as advanced drug delivery systems, Expet Opin. Drug Deliv. 13 (2016) 1609–1623.
[15] Y. Iwao, I. Tomiguchi, A. Domura, Y. Mantaira, A. Minami, T. Suzuki, T. Ikawa, S. I. Kimura, S. Itai, Inflamed site-specific drug delivery system based on the interaction of human serum albumin nanoparticles with myeloperoxidase in a murine model of experimental colitis, Eur. J. Pharm. Biopharm. 125 (2018) 141–147.
[16] S. Gelperina, K. Kisich, M.D. Iseman, L. Heifets, The potential advantages of nanoparticle drug delivery systems in chemotherapy of tuberculosis, Am. J. Respir. Crit. Care Med. 172 (2005) 1487–1490.
[17] L. Yang, F. Cui, D. Cun, A. Tao, K. Shi, W. Lin, Preparation, characterization and biodistribution of the lactone form of 10-hydroxycamptothecin (HCPT)-loaded bovine serum albumin (BSA) nanoparticles, Int. J. Pharm. 340 (2007) 163–172.
[18] F. Crisante, I. Francolini, M. Bellusci, A. Martinelli, L. D'Ilario, A. Piozzi, Antibiotic delivery polyurethanes containing albumin and polyallylamine nanoparticles, Eur. J. Pharmaceut. Sci. 36 (2009) 555–564.
[19] K.R. Shankar, R.K. Ameta, M. Singh, Preparation of BSA nanoparticles using aqueous urea at T=308.15, 313.15 and 318.15 K as a function of temperature, J. Mol. Liq. 216 (2016) 808–813.
[20] B. Demirkurt, Y. Akdogan, Development of an ionic liquid based method for the preparation of albumin nanoparticles, ChemistrySelect 3 (2018) 9940–9945.
[21] B. Demirkurt, G. Cakan-Akdogan, Y. Akdogan, Preparation of albumin nanoparticles in water-in-ionic liquid microemulsions, J. Mol. Liq. 295 (2019), 111713.
[22] N. Desai, Nanoparticle albumin-bound paclitaxel (Abraxane®), in: M. Otagiri, V. Chuang (Eds.), Albumin in Medicine, Springer, Singapore, 2016.
[23] K. Langer, S. Balthasar, V. Vogel, N. Dinauer, H. Von Briesen, D. Schubert, Optimization of the preparation process for human serum albumin (HSA) nanoparticles, Int. J. Pharm. 257 (2003) 169–180.
[24] B. Von Storp, A. Engel, A. Boeker, M. Ploeger, K. Langer, Albumin nanoparticles with predictable size by desolvation procedure, J. Microencapsul. 29 (2012) 138–146.
[25] Z. Kayani, O. Firuzi, A.-K. Bordbar, Doughnut-shaped bovine serum albumin nanoparticles loaded with doxorubicin for overcoming multidrug-resistance in cancer cells, Int. J. Biol. Macromol. 107 (2018) 1835–1843.
[26] H.H. Nguyen, J. Ryu, J.-H. Che, T.S. Kang, J.K. Lee, C.W. Song, S. Ko, Robust size control of bovine serum albumin (BSA) nanoparticles by intermittent addition of a desolvating agent and the particle formation mechanism, Food Chem. 141 (2013) 695–701.
[27] F. Galisteo-González, J. Molina-Bolívar, Systematic study on the preparation of BSA nanoparticles, Colloids Surf., B 123 (2014) 286–292.
[28] S. Sun, Q-Ru Xiao, Y. Wang, Y. Jiang, Roles of alcohol desolvating agents on the size control of bovine serum albumin nanoparticles in drug delivery system, J. Drug Deliv. Sci. Technol. 47 (2018) 193–199.
[29] M. Akbarian, N. Ebtekar, Z. Pakravan, M. Hassan, Folate receptor alpha targeted delivery of artemether to breast cancer cells with folate-decorated human serum albumin nanoparticles, Int. J. Biol. Macromol. (2020), https://doi.org/10.1016/j.ijbiomac.2020.02.106.
[30] J.Y. Jun, H.H. Nguyen, H.S. Chun, B.C. Kang, S. Ko, Preparation of size-controlled bovine serum albumin (BSA) nanoparticles by a modified desolvation method, Food Chem. 127 (2011) 1892–1898.
[31] H.J. Byeon, L.Q. Thao, S. Lee, S.Y. Min, E.S. Lee, B.S. Shin, H.-G. Choi, Y.S. Youn, Doxorubicin-loaded nanoparticles consisted of cationic- and mannose-modified-albumins for dual-targeting in brain tumors, J. Contr. Release 225 (2016) 301–313.
[32] M.A. Martinez-Gomez, S. Sagrado, R.M. Villanueva-Camanas, M.J. Medina-Hernandez, Characterization of basic drug-human serum protein interactions by capillary electrophoresis, Electrophoresis 27 (2006) 3410–3419.
[33] D. Tatlidil, M. Ucuncu, Y. Akdogan, Physiological concentrations of albumin favor drug binding, Phys. Chem. Chem. Phys. 17 (2015) 22678–22685.
[34] Y. Akdogan, M. Emrullahoglu, D. Tatlidil, M. Ucuncu, G. Cakan-Akdogan, EPR studies of intermolecular interactions and competitive binding of drugs in a drug–BSA binding model, Phys. Chem. Chem. Phys. 18 (2016) 22531–22539.
[35] A. Verma, F. Stellacci, Effect of surface properties on nanoparticle- cell interactions, Small 6 (2010) 12–21.
[36] S. Abbasi, A. Paul, W. Shao, S. Prakash, Cationic albumin nanoparticles for enhanced drug delivery to treat breast cancer: preparation and in vitro assessment, J. Drug Deliv. 2012 (2012), 686108.
[37] A. Saha, N. Pradhan, S. Chatterjee, R.K. Singh, V. Trivedi, A. Bhattacharyya, D. Manna, Fatty-amine-conjugated cationic bovine serum albumin nanoparticles for target-specific hydrophobic drug delivery, ACS Appl. Nano Mater. 2 (2019) 3671–3683.
[38] J. Han, Q. Wang, Z. Zhang, T. Gong, X. Sun, Cationic bovine serum abumin based self-assembled nanoparticles as siRNA delivery vector for treating lung metastatic cancer, Small 10 (2014) 524–535.
[39] Y. Akdogan, Y. Wu, K. Eisele, M. Schaz, T. Weil, D. Hinderberger, Host–guest interactions in polycationic human serum albumin bioconjugates, Soft Mater. 8 (2012) 11106–11114.
[40] K. Eisele, R.A. Gropeanu, C.M. Zehendner, A. Rouhanipour, A. Ramanathan, G. Mihov, K. Koynov, C.R.W. Kuhlmann, S.G. Vasudevan, H.J. Luhmann, T. Weil, Fine-tuning DNA/albumin polyelectrolyte interactions to produce the efficient transfection agent cBSA-147, Biomaterials 31 (2010) 8789–8801.
[41] E. Cheraghipour, S. Javadpour, Cationic albumin-conjugated magnetite nanoparticles, novel candidate for hyperthermia cancer therapy, Int. J. Hyperther. 29 (2013) 511–519.
[42] J.N. Lee, C. Park, G.M. Whitesides, Solvent compatibility of poly (dimethylsiloxane)-based microfluidic devices, Anal. Chem. 75 (2003) 6544–6554.
[43] H.A. Rizk, I.M. Elanwa, Dipole moments of glycerol, isopropyl alcohol, and isobutyl alcohol, Can. J. Chem. 46 (1968) 507–513.
[44] H. Mohammad-Beigi, S.A. Shojaosadati, D. Morshedi, N. Mirzazadeh, A. Arpanaei, The effects of organic solvents on the physicochemical properties of human serum albumin nanoparticles, Iran. J. Biotechnol. 14 (2016) 45–50.
[45] R. Sadeghi, A.A. Moosavi-Movahedi, Z. Emam-Jomeh, A. Kalbasi, S.H. Razavi, M. Karimi, J. Kokini, The effect of different desolvating agents on BSA nanoparticle properties and encapsulation of curcumin, J. Nanoparticle Res. 16 (2014) 1–14.
[46] L.F. He, D.L. Lin, Y.Q. Li, Micelle–sensitized constant-energy synchronous fluorescence spectrometry for the simultaneous determination of pyrene, benzo[*a*] pyrene and perylene, Anal. Sci. 21 (2005) 641–645.
[47] R. Liu, P. Qin, L. Wang, X. Zhao, Y. Liu, X. Hao, Toxic effects of ethanol on bovine serum albumin, J. Biocem. Mol. Toxicol. 24 (2010) 66–71.
[48] K. Karami, N. Jamshidian, A. Hajiaghasi, Z. Amirghofran, BSA nanoparticles as controlled release carriers for isophethalaldoxime palladacycle complex; synthesis, characterization, in vitro evaluation, cytotoxicity and release kinetics analysis, New J. Chem. 44 (2020) 4394–4405.
[49] P.L. Ritger, N.A. Peppas, A simple equation for description of solute release II. Fickian and anomalous release from swellable devices, J. Contr. Release 5 (1987) 37–42.
[50] E. Fröhlich, The role of surface charge in cellular uptake and cytotoxicity of medical nanoparticles, Int. J. Nanomed. 7 (2012) 5577–5591.